

Incandescent metasurfaces: A tutorial



Cite as: APL Photon. 9, 111101 (2024); doi: 10.1063/5.0223889

Submitted: 18 June 2024 • Accepted: 17 October 2024 •

Published Online: 4 November 2024



Jean-Jacques Greffet,^{1,a)} Benjamin Vest,¹ Patrick Bouchon,² and Bo Zhao³

AFFILIATIONS

¹ Université Paris-Saclay, Institut d'Optique Graduate School, CNRS, Lab. Charles Fabry, Palaiseau, France

² DOTA, ONERA, Université Paris-Saclay, Palaiseau, France

³ Department of Mechanical and Aerospace Engineering, University of Houston, Houston, Texas 77004, USA

Note: This paper is part of the APL Photonics Special Topic on Mid-IR Photonics.

a) Author to whom correspondence should be addressed: jean-jacques.greffet@institutoptique.fr

ABSTRACT

Incandescence has long been the most popular source of light, despite a number of limitations in terms of efficiency, polarization, and coherence. In the last twenty years, it has been shown that most of these limitations can be overcome by taking advantage of the advances in nanophotonics. In this paper, we provide a tutorial presentation of the field with emphasis on the fundamental principles used to control the properties of thermal radiation in the far field. We introduce several figures of merit and list some directions for future work.

© 2024 Author(s). All article content, except where otherwise noted, is licensed under a Creative Commons Attribution-NonCommercial 4.0 International (CC BY-NC) license (<https://creativecommons.org/licenses/by-nc/4.0/>). <https://doi.org/10.1063/5.0223889>

I. INTRODUCTION

The purpose of this paper is to review recent advances in the control of thermal emission by hot bodies, also known as incandescence. Incandescence is often associated with a number of features. First, the spectrum is usually assumed to be like the blackbody spectrum, very broad. We remind you that the blackbody spectrum has a peak wavelength $\lambda_p(T)$ satisfying $\lambda_p(T) \cdot T = 2898 \text{ } \mu\text{m K}$, and 98% of the emitted energy is within the range $[\lambda_p/2; 7\lambda_p]$. The emission is quasi-isotropic and unpolarized except close to the Brewster angle. The radiation emitted by a large body cannot be modulated rapidly due to its thermal inertia. The wall-plug efficiency is low. For instance, a light bulb has an efficiency on the order of 0.03, much smaller than the efficiency of a light-emitting diode. Finally, the spectral radiance of the source, namely, the power emitted in an optical etendue $dS \cos(\theta) d\Omega$ and a spectral range $d\omega$, is much lower than for lasers. While all these features are very familiar, only the last one is enforced by the laws of physics. The spectral radiance in vacuum is given by $(c/4\pi) (\omega^2/\pi^2 c^3) n(\omega) \hbar\omega$, where $n(\omega)$ is the number of photons in a mode and $\omega^2/\pi^2 c^3$ is the density of states. For a body at temperature T , $n(\omega)$ is given by the Bose-Einstein distribution $n^{BE}(\omega, T) = 1/[\exp(\hbar\omega/k_B T) - 1]$, which is bounded by $k_B T/\hbar\omega$ at high temperature. It turns out that all the other features of the light emitted by an incandescent source can be engineered. It is possible to design directional and monochromatic thermal sources. The emitted power can be polarized, and the conversion of heat into

radiation can be made very efficient. Fast modulation of the emitted power is also possible. The purpose of this paper is to give an introduction to the key ideas that can be implemented to tailor light emission by incandescent sources.

In Sec. II, we remind you of the basic concepts of radiometry, which is a phenomenological framework to describe radiative fluxes. We then introduce an alternative model based on Maxwell equations that establishes a connection with the electrical engineer's point of view on the emission of electromagnetic waves by time-dependent currents in antennas. In the case of thermal radiation, the time-dependent currents that emit light are the time-dependent thermodynamic fluctuations of the current density. They can be computed with a statistical physics approach. This alternative framework is called fluctuational electrodynamics. It provides an extension of the radiometric results beyond the geometrical optics domain of validity.

When designing emission properties, Kirchhoff's law plays a central role. Kirchhoff showed in 1860 that the power emitted by an incandescent body can be cast as the product of its absorptivity by a universal function of frequency and temperature that is at present known as blackbody radiance.¹ Although the law was first derived in the framework of geometrical optics, its validity at the nanoscale has been later proved in the framework of fluctuational electrodynamics. Hence, all the properties of the emitted radiation in terms of emission spectrum, directivity, and polarization are described by the absorptivity. Controlling these properties amounts to design the

absorptivity of the body. We will provide a qualitative introduction to the physical origin of this law and discuss its implications. In particular, this will be useful to grasp how an incandescent source can produce temporally and spatially coherent radiation. In his derivation, Kirchhoff used the concept of absorptivity of a homogeneous medium separated from vacuum by a planar interface. Hence, there is only one degree of freedom to control the absorptivity, the refractive index. We know that any periodic material with a period smaller than half a wavelength behaves as an effective material with a given absorptivity. In marked contrast with a homogeneous medium, such a medium that we call a metamaterial can be made of several materials and may have a large variety of geometrical structures. This provides an arbitrary large number of degrees of freedom to engineer the absorptivity. Remarkably, it is not necessary to develop a bulk metamaterial to control absorption. A metamaterial layer with a thickness smaller than the wavelength is sufficient to tailor absorptivity. When heated to generate thermal emission, it is called thermal metasurface or incandescent metasurface. In practice, most of the metasurfaces belong to three classes: (i) arrays of non-interacting plasmonic or dielectric resonators supporting localized modes, (ii) metasurfaces sustaining delocalized modes such as surface lattice resonances in arrays of coupled resonators, surface plasmons or planar waveguide modes used in conjunction with corrugations to tailor their radiative leakage, and (iii) stacks of multilayers.

The paper starts with a summary of basic concepts covering radiometry, fluctuational electrodynamics, Kirchhoff's law, and coherence. We then discuss how to design incandescent metasurfaces to control directivity in Sec. III, emission spectrum in Sec. IV, polarization in Sec. V, efficiency in Sec. VI, and how to modulate the amplitude in Sec. VII. We discuss the case of nonreciprocal materials so that Kirchhoff's law cannot be used in Sec. VIII. Section IX briefly addresses the use of a generalized Kirchhoff's law to design sources in nonequilibrium situations beyond incandescence. The aim of this paper is to provide a tutorial introduction to the field; it does not attempt to review the abundant literature, which has been very well covered by recent reviews.²⁻⁷ We focus on the basic physical mechanisms and on the figure of merits to characterize the emitter properties.

II. THERMAL RADIATION: BASIC CONCEPTS

A. The radiometric approach

In radiometry, the power dQ emitted by an elementary opaque surface dS at temperature T in an elementary frequency range $d\omega$ around the circular frequency ω in a solid angle $d\Omega$ around a direction \mathbf{u} making an angle θ with the normal to the surface is given by

$$dQ(\omega, \theta) = I_\omega^e(T) dS \cos \theta d\omega d\Omega, \quad (1)$$

where $I_\omega^e(T)$ is the radiance (or specific intensity) of the emitted radiation (see Fig. 1). The radiance leaving the body is the sum of the emitted and reflected radiances, which are both positive. At thermodynamic equilibrium, the radiance is given by the universal form

$$I_{BB,\omega}(T) = \frac{c}{4\pi} \times \frac{\omega^2}{\pi^2 c^3} \times \frac{\hbar\omega}{\exp(\hbar\omega/k_B T) - 1}, \quad (2)$$

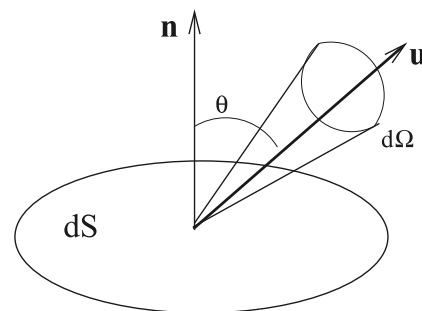


FIG. 1. Notations used to describe the field radiated through an area dS in the solid angle $d\Omega$.

also known as blackbody radiance or blackbody luminance. In this equation, the second term is the density of electromagnetic modes in vacuum, and the third is the mean energy per mode, so their product is the energy per unit volume at equilibrium. The first term relates the specific intensity to the energy per unit volume. We now explain the origin of the name blackbody. The concept of a blackbody was introduced by Kirchhoff,¹ who defined it as a body that absorbs all incident radiation so that there is no reflection. The radiance leaving a blackbody is thus equal to the emitted radiance. At thermodynamic equilibrium, it has to be equal to I_{BB} . Consequently, the emitted radiance by a blackbody at temperature T is $I_{BB}(T)$, and the radiance emitted by an arbitrary radiant body is a fraction of $I_{BB}(T)$ and can be cast in the form

$$I_\omega^e(T) = E(\omega, \theta) I_{BB,\omega}(T), \quad (3)$$

where $E(\omega, \theta)$ is the emissivity (a positive number smaller than 1). It is important to stress that the radiometric description is based on geometrical optics. It does not account for diffraction and cannot be used for objects with sizes on the order of or smaller than the wavelength.

In what follows, we will be interested in the physical meaning of the emissivity and the different ways to engineer this quantity. Here, we note that the emissivity is a real number between 0 and 1 that depends on frequency and angle. It also depends on polarization. It characterizes the ability of a material to produce thermal radiation. In radiometry, it is introduced as a phenomenological quantity.

B. The fluctuational electrodynamics approach

An alternative description of thermal radiation was introduced by Rytov *et al.*⁸ It is based on Maxwell's equations so that the fields are emitted by time-dependent currents existing in the hot bodies. It is thus necessary to introduce random currents that account for the random motion of charges, be they electrons or ions. Given the linearity of Maxwell's equations, there exists a linear relation between the fields and the sources so that the electric field can be cast in the form of

$$\mathbf{E}^f(\mathbf{r}, \omega) = i\omega\mu_0 \int_V d\mathbf{r}' \mathbf{G}^E(\mathbf{r}, \mathbf{r}', \omega) \cdot \mathbf{j}^f(\mathbf{r}', \omega), \quad (4)$$

where the integral is taken over the volume V , which contains the fluctuating source currents $\mathbf{j}^f(\mathbf{r}', \omega)$, and \mathbf{G}^E is the electric Green

tensor. Note in particular that each volume element can be characterized by a fluctuating dipole \mathbf{p}_f such that $-i\omega\mathbf{p}_f = \mathbf{j}^f(\mathbf{r}', \omega)d\mathbf{r}'$. Consequently, thermal radiation can be reduced to the emission of a set of random time-dependent dipoles located in the volume of the emitter. With this approach, the radiation of light by thermally generated random currents becomes an antenna problem that can be solved using Maxwell's equation solvers. This method is much more powerful than the radiometric approach, which is only valid in the framework of geometrical optics. The fluctuational electrodynamics model can be used for subwavelength objects or nanostructures; it can account for diffraction and interferences.

To proceed, it is necessary to have an explicit model of the fluctuating currents. On average, the current is zero, so the average emitted field is zero. However, the quantity of interest is the flux of the Poynting vector, which is a quadratic quantity. Hence, we need to know the correlation function of the fluctuating current. We first assume that the statistical properties of the current density are time-independent or, in other words, that the process is stationary. The consequence is that the correlation function can be cast in the form

$$\langle j_n^f(\mathbf{r}, \omega) j_m^f(\mathbf{r}', \omega') \rangle = 2\pi\delta(\omega + \omega') W_{j_n j_m}(\mathbf{r}, \mathbf{r}', \omega), \quad (5)$$

where the delta function $2\pi\delta(\omega + \omega')$ accounts for the stationarity of the system and $W_{j_n j_m}(\mathbf{r}, \mathbf{r}', \omega)$ is the power spectral density.⁹ Note that $j_m^f(t)$ is real so that $j_m^f(\mathbf{r}', -\omega) = j_m^f(\mathbf{r}', \omega)$. The power spectral density of the current density fluctuation is given at thermodynamic equilibrium by the fluctuation-dissipation theorem,¹⁰

$$W_{j_n j_m}(\mathbf{r}, \mathbf{r}', \omega) = \omega \epsilon_0 i [\epsilon_{mn}^*(\omega) - \epsilon_{nm}(\omega)] \Theta(\omega, T) \delta(\mathbf{r} - \mathbf{r}'), \quad (6)$$

where $i^2 = -1$, $j_n^f(\mathbf{r}, \omega)$ is a spatial component of the fluctuating current density at the frequency ω . The subscripts n or m stand for the x , y , or z components of the vector. $\epsilon_{nm}(\omega)$ is the local relative permittivity tensor of the emitter and the function

$$\Theta(\omega, T) = \frac{\hbar\omega}{2} + \frac{\hbar\omega}{e^{\hbar\omega/(k_B T)} - 1} \quad (7)$$

is the mean energy of a harmonic oscillator with frequency ω in thermodynamic equilibrium with a heat bath at temperature T . k_B is Boltzmann constant and $2\pi\hbar$ is Planck constant. We note that the presence of the term $\delta(\mathbf{r} - \mathbf{r}')$ in Eq. (6) is a consequence of the assumption of a local medium. The theorem is given for anisotropic media and can be simplified for an isotropic medium using $\epsilon_{nm}(\omega) = \epsilon(\omega)\delta_{nm}$. This theorem is valid for both reciprocal [$\epsilon_{mn}(\omega) = \epsilon_{nm}(\omega)$] and nonreciprocal media [$\epsilon_{mn}(\omega) \neq \epsilon_{nm}(\omega)$].

It is seen that the correlation of the current density in an isotropic medium is proportional to $\text{Im}[\epsilon(\omega)]$, which accounts for the dissipation. Let us remember that the rate of losses in a material is given by $\omega\epsilon_0\text{Im}[\epsilon(\omega)]|E|^2/2$. Consequently, the emitted spectrum is governed by the absorption spectrum. Therefore, emission can only take place in an absorbing medium. This may seem counter-intuitive, as it is often assumed that light does not penetrate an opaque medium and that both emission and absorption are surface processes. The fluctuational electrodynamics formalism clearly indicates that emission and absorption are volume processes. Let us consider light emission by a half-space filled with a hot metal as an example. The fluctuational electrodynamics model accounts for emission by the random movement of electrons in the bulk of the

sample. Due to the small propagation length, the emitted fields cannot propagate very far and are reabsorbed over very short distances. In other words, there are photons in metal. From the thermodynamic point of view, this is not surprising. At equilibrium, all forms of energy in a system, be they electronic, vibrational, or electromagnetic, are excited. The fields emitted in vacuum by the metallic body are due to the emitters which are close to the vacuum-metal interface in the so-called skin-depth.

C. Kirchhoff's law in a nutshell

Kirchhoff showed in 1860 that the emissivity E is equal to the absorptivity A .¹ This is a remarkable relation, as the emissivity is introduced from energy and thermodynamics arguments, whereas absorptivity can be computed in the framework of coherent optics using plane waves illuminating bodies. Kirchhoff's law is thus a bridge between the world of radiometry and thermodynamics on the one hand and the world of coherent optics on the other hand. Absorptivity can be engineered using interference or resonant structures. As a consequence, a design of absorptivity using coherent optics amounts to design the emissivity and, therefore, to control thermal radiation. Hence, Kirchhoff's law is a very powerful tool to design emission properties. The argument of Kirchhoff was based on energy budget, ray absorption, and emission, so the validity of the result for resonant and diffractive surfaces is not obvious. Derivations based on fluctuational electrodynamics^{8,11} and also on reciprocity properties of the scattering matrix for fields¹² have enabled us to prove its validity beyond the geometrical optics regime.

To get some physical insight on this remarkable property, we provide a qualitative discussion of the emissivity and absorptivity of a semi-infinite absorbing medium depicted in Fig. 2. We consider either a situation where a beam is impinging on a plane surface with a given polarization, a given frequency, and a given angle [Fig. 2(a)] or a situation where we consider thermal emission in the same direction, frequency, and polarization [Fig. 2(b)]. We first consider the case of a beam incident on the interface coming from vacuum (medium 1). The corresponding energy is either specularly reflected or transmitted by the interface with a transmission factor T_{12} . We note that the energy transmitted by the interface is absorbed in medium 2 as it propagates. As medium 2 is considered to be a half space, all the energy transmitted by the interface is eventually absorbed. Therefore, we conclude that the absorptivity is nothing but the interface transmission $A = T_{12}$.

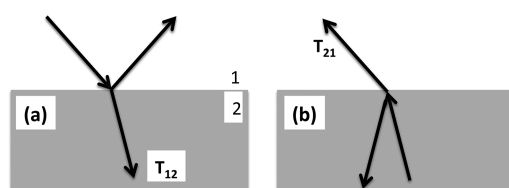


FIG. 2. Kirchhoff law: (a) An incident beam is either reflected or transmitted by the plane interface. Transmitted light is subsequently absorbed in the opaque body (2). (b) The light emitted by the hot body is transmitted by the interface. The equality between absorption and emission follows from the equality $T_{12} = T_{21}$.

We now consider the emission by the lower half-space in local thermodynamic equilibrium with temperature T [see Fig. 2(b)]. While the medium is opaque, it contains charges (ions, electrons), which are randomly moving in the system and, therefore, radiate. The corresponding radiation is in local thermodynamic equilibrium with other excitations such as electrons and phonons. It is thus characterized by blackbody radiation at the temperature of the body, as discussed in Sec. II A. Obviously, radiation cannot propagate over long distances as the medium is lossy. The typical decay length is the skin depth. Nevertheless, photons emitted within a distance to the interface smaller than the skin depth can be transmitted through the interface. Once these photons are transmitted by the interface, they are considered to be emitted. Hence, we conclude that the emission is proportional to the transmission factor T_{21} . Now, it can be shown using the reciprocity theorem that the transmission factor of the interface satisfies the equality $T_{12} = T_{21}$ provided that the materials are reciprocal, namely, that $\epsilon_{ij} = \epsilon_{ji}$. The equality $T_{12} = T_{21}$ is the physical origin of Kirchhoff's law: both absorptivity and emissivity are in fact nothing but transmission by an interface. With this physical picture in mind, it now appears that engineering thermal emission amounts to tailor the interface transmission factor. It is well known that this can be achieved using coatings or multilayers. It can also be performed using metasurfaces or tailoring radiative leakages of surface waves for example. All these systems enable us to tailor the absorption as a function of frequency, angle, and polarization.

We now briefly analyze what is needed to have an emitter with an emissivity approaching 1. It is clear from the previous discussion that we need an opaque medium with a transmission factor equal to 1. At normal incidence, the transmission factor for energy is given by $T_{21} = 1 - R_{22} = 1 - \left| \frac{n-1}{n+1} \right|$. In order to cancel the reflectivity, we need $n = 1$. As the medium must be absorbing to be opaque, the ideal absorber should have an index of the form $1 + i\eta$ with $\eta \ll 1$. For dispersive crystals, this index matching condition is satisfied in the infrared part of the spectrum at the so-called Christiansen frequency. This particular frequency is often used to normalize an emissivity spectrum.¹³

We finally comment on the influence on the emissivity of the density of electromagnetic states in the emitting body. While an increase in this density enables to increase the energy per unit volume inside the emitting body, it does not increase the emission. To understand this point, let us consider as an example emission in vacuum by a hot material in a half-space ($z < 0$) with refractive index $n = n' + in''$. The larger n' , the larger the number of modes per unit volume in the emitting body given by $n'^3 \omega^2 / (\pi^2 c^3)$. Nevertheless, all the modes with a propagation direction fulfilling the condition $n' \sin(\theta) > 1$ are totally reflected at the interface medium-vacuum so that their transmission factor is zero. The additional modes cannot contribute to the emission. In summary, increasing the energy density inside an emitter by increasing the local density of states does not produce an increase of the emitted power in vacuum.

D. Absorptivity, absorption cross section, absorption rate, and local Kirchhoff's law

In Sec. II C, we have introduced the absorptivity A of an opaque body, which is the ratio $|S_{n,t}/S_{n,inc}|$ of the transmitted and incident normal components of the Poynting vector. As discussed earlier, it is the intensity transmission factor that can be computed with Fresnel

formulas. This quantity is defined for a plane wave impinging on an infinite planar surface. It can be used locally on a surface inasmuch as a finite size beam is well collimated. If we consider a focused beam with a diameter on the order of or smaller than a wavelength, the beam is a superposition of different plane waves with different transmission factors so that the absorptivity is not given by the Fresnel factor. Similarly, when dealing with a subwavelength body, a Fresnel reflection factor cannot be defined. However, it is always possible to compute the total absorbed power P_{abs} using a full solution of Maxwell's equations. It can be cast in the form^{9,14}

$$P_{abs} = \sigma_{abs}(\mathbf{u}, \omega, l) \phi_{inc}, \quad (8)$$

where σ_{abs} is the absorption cross section and ϕ_{inc} is the power per unit area of the incident plane wave. It is seen that the absorption cross section has the dimension of an area. If the object is very large compared to the skin depth and the wavelength, this absorption cross section can be derived from a surface integral of the absorptivity. However, for subwavelength objects, the concept of absorptivity cannot be used, and there is no simple relation between the absorption cross section and the area of the object. Nonetheless, Kirchhoff's law can still be expressed using the absorption cross section. The power emitted by an arbitrary particle in a solid angle $d\Omega$ with polarization l can be cast in the form^{8,11}

$$P_e^{(l)} = \sigma_{abs}(-\mathbf{u}, \omega, l) \frac{I_{BB,\omega}(T)}{2} d\Omega. \quad (9)$$

It is possible to introduce a local absorption rate $dP_{abs} = \alpha(-\mathbf{u}, \omega, l, \mathbf{r}) \phi_{inc} d^3 \mathbf{r}$ so that

$$\sigma_{abs}(-\mathbf{u}, \omega, l) = \int_V \alpha(-\mathbf{u}, \omega, l, \mathbf{r}) d^3 \mathbf{r}. \quad (10)$$

Using this local form of absorption, it is possible to introduce a local form of Kirchhoff's law. This enables us to extend Kirchhoff's law to anisothermal bodies where the temperature field is $T(\mathbf{r})$ ^{11,15}

$$P_e^{(l)} = \int_V \alpha(-\mathbf{u}, \omega, l, \mathbf{r}) \frac{I_{BB,\omega}(T(\mathbf{r}))}{2} d^3 \mathbf{r} d\Omega. \quad (11)$$

To conclude this section, we stress that the radiometric point of view is no longer valid at the nanoscale. Nevertheless, Kirchhoff's law is still valid for subwavelength particles, provided that the absorption cross section is used to compute the emission and absorption.

E. Spatial and temporal coherence

Before addressing the different techniques that enable to control the features of radiation, we briefly discuss the connection between narrow spectrum and temporal coherence on the one hand and between directivity and spatial coherence on the other hand. It is indeed possible to design partially spatial and temporally coherent thermal sources, something that is counterintuitive given that blackbody radiation is often used as the overarching example of incoherent light.

For the sake of simplicity, we deal with a scalar field $E(\mathbf{r}, t)$. As the sources are random, the field is a random process. We assume that it is stationary and homogeneous so that its statistical properties are translationally invariant in time and space. We introduce the correlation function $\langle E(\mathbf{r}_1, t_1)E(\mathbf{r}_2, t_2) \rangle = C(\mathbf{r}_1 - \mathbf{r}_2, t_1 - t_2)$ which

contains all the information on the field coherence. The temporal coherence is characterized by the correlation function at a given point and two different times $\langle E(\mathbf{r}, t_1)E(\mathbf{r}, t_2) \rangle$ whereas the spatial coherence is characterized by the cross correlation function, which is the correlation function at two points and a given time $\langle E(\mathbf{r}_1, t)E(\mathbf{r}_2, t) \rangle$ or by the cross spectral density $\langle E(\mathbf{r}_1, \omega)E(\mathbf{r}_2, \omega) \rangle$ in frequency domain. A random field is temporally coherent if the correlation time is much larger than the field period; the field is spatially coherent if the correlation length is much larger than the wavelength.

It turns out that there is a mathematical connection between the time correlation function of a stationary process and its spectrum. It is given by the Wiener–Khinchin theorem. For the temporal coherence, it can be cast in the form

$$\langle E(\mathbf{r}_1, t_1)E(\mathbf{r}_1, t_2) \rangle = \int_{-\infty}^{\infty} \frac{d\omega}{2\pi} W_{EE}(\mathbf{r}_1, \mathbf{r}_1, \omega) \exp[-i\omega(t_1 - t_2)], \quad (12)$$

where $W_{EE}(\mathbf{r}_1, \mathbf{r}_1, \omega)$ is the power spectral density of the field.⁹ According to the Fourier transform properties, a long correlation time corresponds to a narrow spectrum. Hence, the temporal coherence can be increased by reducing the spectral width of a random field. The Wiener–Khinchin theorem applied to the space variables x, y in the plane $z = 0$ at the surface of the source leads to

$$\begin{aligned} \langle E(\mathbf{r}_1, \omega)E^*(\mathbf{r}_2, \omega) \rangle &= \int_{-\infty}^{\infty} \frac{dk_x}{2\pi} \int_{-\infty}^{\infty} \frac{dk_y}{2\pi} W_{EE}(k_x, k_y, z=0, \omega) \\ &\quad \times \exp[ik_x(x_1 - x_2) + ik_y(y_1 - y_2)]. \end{aligned} \quad (13)$$

Here again, the properties of a Fourier transform indicate that a power spectral density with a narrow extension in k_x and k_y , namely a directional beam, corresponds to a *large spatial coherence length in the source plane $z = 0$* . Importantly, $W_{EE}(k_x, k_y, z = 0, \omega)$ is proportional to the emitted radiance^{16,17} so that there is a direct Fourier transform connection between the angular dependence of the radiance and the spatial correlation function in the source plane.

Note that this relation differs from the van Cittert–Zernike theorem, which is often cited when discussing spatial coherence.¹⁸ The later does not address the issue of spatial coherence in the plane $z = 0$ of the source but rather the spatial coherence in a plane $z = z_0$ in the far-field region illuminated by an incoherent source (the field is delta correlated in the source plane) with transverse size L . The far-field region is defined by $z_0 \gg L^2/\lambda$ and $z_0 \gg \lambda$. The van Cittert–Zernike theorem states that there is a transverse coherence length given by $\lambda(L/z_0)$ in the plane $z = z_0$. This relation shows that the field produced by any incoherent source becomes partially coherent in the far field.

In summary, the coherence can be increased by filtering the spectrum using a narrow passband filter (either in ω for temporal coherence or in k for spatial coherence). Hence, nothing prevents a hot body to emit partially coherent radiation. According to the qualitative discussion on Kirchhoff's law, it suffices to design a structure whose transmissivity is large in a narrow frequency interval $\Delta\omega$ to emit partially temporally coherent light or in a narrow wavevector interval $\Delta k_x \Delta k_y$ to emit a partially spatially coherent light. Obviously, by doing so, the number of modes contributing to the emission is reduced and, therefore, the emitted power is reduced. It can be increased by either increasing the temperature or the emitting area.

One could think that if the emitted energy could be conserved while redirecting this energy into a narrow solid angle, then the radiance emitted by a body at temperature T could be increased. In principle, it is possible to design an emitter operating at constant flux instead of constant temperature. It should absorb a constant flux, be perfectly isolated, and have only radiative losses so that the emitted power would equal the absorbed power. Then, the emitter temperature would increase as the number of emitting modes was reduced, but the emitted power would be constant. If the temperature of the body is kept constant and the number of emitting modes is reduced, the flux is simply reduced because the number of photons in a mode is given by the Bose–Einstein distribution, which only depends on the temperature.

We have seen that it is possible to increase the temporal coherence by merely filtering the emitted radiation and reducing the bandwidth. Hence, why not simply filter the radiation emitted by a blackbody? To address this question, we compare a hot body whose emissivity is zero for all frequencies except in a narrowband centered on ω_0 with a blackbody at the same temperature emitting at all frequencies through a passband filter centered on ω_0 . Both systems emit radiation that is partially temporally coherent. The filtered broadband emitter has a very low efficiency, as only a tiny fraction of the emitted power is transmitted by the filter. In contrast, the narrowband thermal emitter only emits at the useful frequency, so it requires much less energy. We can repeat the same discussion with spatial coherence. Quasi isotropic emission could be collimated using a pinhole in a Fourier plane at the expense of rejecting most of the energy emitted in other directions. For better efficiency, it is thus of interest to design incandescent sources that emit at a narrow solid angle and at the required frequencies.

III. TAILORING THE DIRECTIVITY

As discussed in Sec. II, the directivity of an emitting surface can be tailored by controlling the transmission factor of the interface between a material and vacuum. In order to generate a directional emitter, it is necessary to design a transmission factor that approaches zero for all directions except a small solid angle. The question is thus to find a methodology to design such surfaces. The first demonstration of a clear and large spatial coherence was achieved with a grating ruled on a SiC surface.¹⁹ A SiC surface is highly reflective for all angles and, therefore, has a low emissivity. By ruling a grating with period d on its surface, it is possible to couple surface phonon polariton whose dispersion relation is given by $k_{x,sp}(\omega)$ to plane waves in vacuum. By properly designing the grating amplitude and period, it is possible to obtain total absorption for a well-defined angle and frequency such that $k_{x,sp}(\omega) = k_{x,inc} + 2\pi/d$ (see Fig. 3). According to Kirchhoff's law, this grating emits at a well-defined angle and frequency. The measurements of emission show a good agreement between absorptivity calculations and emission data (right panel of Fig. 3).

Let us now infer some general rules from this example. We started with a plane interface between a material and vacuum whose reflectivity is large so that emission is reduced in all directions. We then added a second ingredient, the surface wave, which is a delocalized mode of the interface. We finally added a third ingredient, the grating, which is used to produce and control radiative losses for the surface waves, which thus become leaky waves. The emission

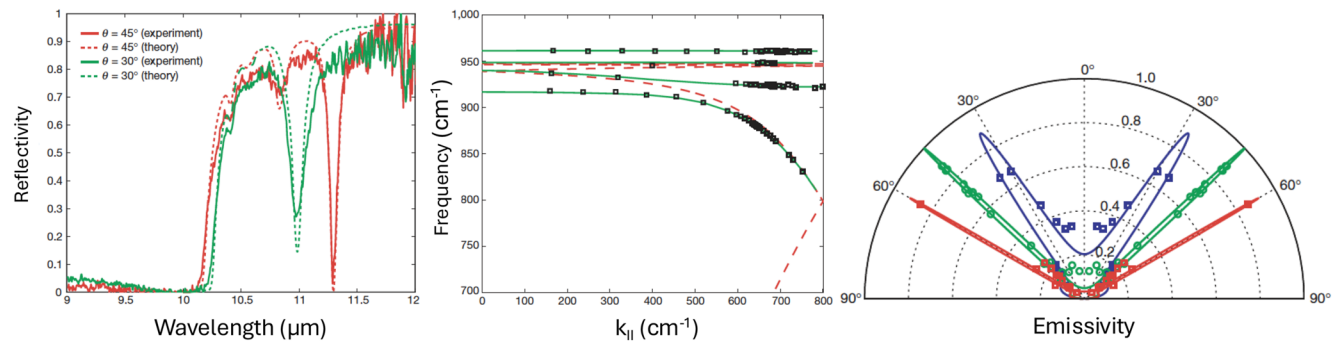


FIG. 3. Directional emission. Left panel: Reflectivity of a SiC grating at 30° and 45° as a function of wavelength showing large absorption dips. Center panel: dispersion relation of the surface phonon polariton obtained by plotting the positions of the reflectivity minima. Right panel: Angular emission pattern for three different wavelengths, absorptivity calculation are shown in plain lines, and experimental data are reported with markers. The three figures are reproduced from Ref. 19.

process can be split in two steps. First, the random thermal currents can excite efficiently the surface mode. Second, the surface mode is scattered by the grating. Hence, the leaky mode behaves as an intermediate cavity coupled to both the sources and the modes of the vacuum. Engineering the emission properties amounts to engineer the radiative losses of the surface wave. This enables us to control the emission direction, frequency, and polarization. With this analysis, it becomes clear that any structure that is coupled to the sources on the one hand and to the plane waves in vacuum on the other hand could be used as an intermediate cavity, enabling to tailor thermal emission.

Let us now discuss in more detail what conditions are required to achieve a highly directional emission pattern. In other words, what are the conditions to control the radiative losses of the “intermediate cavity”? From Eq. (13), we need spatial coherence over a large distance to generate a narrow beam. Hence, the mode of the intermediate cavity introduced previously must be spatially extended in the plane of the source. Light of this mode scattered by small apertures or subwavelength scatterers may produce an interference pattern with a small angular aperture. From basic diffraction theory, it is known that the angular width is given by $\Delta\theta \approx \lambda/L$, where L is the size of the array of scatterers. With these rules in mind, it appears that any leaky mode can be used to generate directional emission. It could be a surface plasmon, a guided wave, or a surface lattice resonance (SLR). The limit to the directivity is the spatial extension of the mode in the plane of the source. It is limited either by the source size or by the decay length of the mode. Instead of producing a single narrow beam, it is possible to arrange the scatterers in the source plane in such a way that they produce more complex patterns or focus in a plane at a finite distance²⁰ from the source.

It is also possible to control the directivity by modifying the efficiency of the coupling to a leaky mode. Here, the idea is that even though the coupling of a surface mode to a plane wave is possible, in practice the amount of radiative losses may be small. The angular pattern may be controlled by controlling this coupling efficiency. The optimum coupling of an incident plane wave to a leaky mode (e.g., a plasmonic mode on a grating or in a waveguide) corresponds to total absorption. To achieve this regime, the critical coupling condition^{9,21} must be satisfied, namely, the radiative losses

of the mode must be equal to its non-radiative losses. This condition is derived in the framework of an approximate model called coupled mode theory. A technique to control the angular width is to ensure that the critical coupling condition is fulfilled in the target angular range only. This approach was used with a plasmonic metasurface, and the angular width could be controlled by modifying the periodicity d of the metasurface.²²

In the example of Fig. 3, the emission is directional in two symmetric directions. To generate a beam in a single direction different from the normal, it is necessary to break the symmetry of the metasurface. A detailed discussion can be found in Ref. 23.

An alternative approach is based on depositing a multilayer system on top of the emitter. Here, the basic concept is then to tailor the interface transmission factor $T(\mathbf{k}, \omega)$ as a function of the emission angle as discussed in Sec. II C. Dielectric multilayers are often used to design spectral filters. They can also be designed to control the angular dependence of the transmission factor.²⁴

Finally, we briefly discuss the possibility of controlling directivity for arbitrary wavelengths. In that case, diffraction should be avoided. Moving away from metasurfaces to non-imaging micro-optics enables us to address this issue. Arrays of microparabolic reflectors with a period of 70 μm have been reported to confine light emission within 16° around the normal direction.²⁵

We now introduce two figures of merit to characterize the directivity of an emitter. The first one is the angular width at half maximum. It depends on the quality factor of the leaky mode. The second one is the fraction of the emitted power that is funneled into the directional peak. Given that the solid angle corresponding to the peak is small, the emission outside the peak must be suppressed. In many cases, the sources have an emissivity approaching 1 in the peak and on the order of 0.1 in the background so that after integrating over all angles, most of the energy is emitted in the background. Reducing this background is still a challenge.

IV. TAILORING THE EMISSION SPECTRUM

A. Narrow lines emission

The use of a leaky wave on a SiC surface led to a directional and quasimonochromatic emission. In that specific case, for each

direction θ , the thermal emission is obtained at a different wavelength according to the dispersion relation, as seen in Fig. 3. It is of course of interest to be able to design a source that emits at a single wavelength for all directions. Let us provide a few guidelines to design such a source. A simple approach is to start with a non-emitting substrate and then to add an array of nanoparticles with a monochromatic absorption spectrum. A non-emitting substrate is either a transparent substrate or a highly reflective substrate. To design the absorption at a given wavelength, it is useful to use resonant nanoparticles whose quality factor will control the spectral width. This could be a metallic nanoparticle with a plasmonic resonance or a dielectric nanoparticle with a Mie resonance. These nanoparticles have a dipolar resonance whose absorption cross section at resonance is universal and takes the value $3\lambda^2/8\pi^3$ regardless of their actual geometrical size inasmuch as they are in the dipolar regime, which is roughly valid for particles smaller than $\lambda/20$. Out of resonance, the absorption cross section decreases significantly.

A simple possibility is to use spherical nanoparticles. However, the tunability of the absorption line is not sufficient, and most plasmonic particles have resonances in the visible. In order to control infrared absorption, one of the most commonly used resonant nanoparticles is the metal–insulator–metal (MIM) resonator.^{22,26–28} We illustrate the operating principle of this resonator in Fig. 4 for the simple case of two stripes periodically repeated with period $d = 5.3 \mu\text{m}$ and different widths. Here, the metal is gold, and the insulator is a thin layer of ZnS. Each stripe behaves as a resonant Fabry–Perot cavity for gap plasmon, which goes back and forth between the two edges. The resonance frequency thus depends on the width w according to $\lambda_r \simeq 2n_{\text{eff}}w$, where n_{eff} is the effective refractive index of the gap plasmon. The peculiarity of the gap plasmon mode is to have a large effective index so that the effective wavelength is much smaller than the wavelength in vacuum. As a result, the MIM resonator is much smaller than the wavelength in vacuum so that it behaves as a resonant and absorbing dipolar particle. Figure 4(b) illustrates that the absorption spectrum has two peaks when using two different stripes with different widths.

Figure 4(c) shows the Poynting vector flow lines for two different frequencies corresponding to the resonances of the gap plasmon mode for each stripe. It is remarkable to observe at resonance the funneling of almost all the incident power into a single resonator. This graphically explains why small resonators, which do not cover the entire available surface, can absorb the entire incident light. Note that power flows through the side of the MIM resonators, penetrates in the gap, and goes to the gold–vacuum interfaces inside the gap to be finally absorbed by gold. Should we have used a lossy material for the spacer, losses could have taken place in this material. We stress that the sizes of the resonators and the period are subwavelength, so geometrical optics is not valid. Nevertheless, it is possible to define the absorption cross section of each stripe.

While we have used two-dimensional (2D) stripes for the sake of simplicity, 2D arrays of particles are often used.^{22,26–28} When designing an array of nanoparticles, the question of the surface density of particles arises. On one hand, it is necessary to increase the area density of the particles to increase the absorption. On the other hand, for a very large density, the interaction between particles could modify the absorption spectrum. In practice, the optical modes of a periodic lattice can be constructed as a linear combination of the particle modes in analogy with the electronic modes of a crystal, which are constructed as a linear combination of atomic modes in the tight binding model. Provided that the interaction between neighboring particles is not too large, the absorption resonance shift remains limited. To achieve an absorption approaching unity, a good rule of thumb is to choose a surface density larger than $1/\sigma_{\text{abs}}$ so that all the incident power can be captured by the array of particles. Given that the absorption cross section at resonance is much larger than the actual size of the particle, it is not difficult to reach an absorptivity larger than one. It is even possible to introduce several different types of nanoparticles to produce several absorption peaks. In the example prepared for this tutorial (see Fig. 4), we have optimized the design so that the absorption is above 0.99 for both resonances. Finally, we plot the distribution of the modulus of the magnetic field $|H_y|$ in the near field. It is seen that the field is concentrated in the volume of the gap of the MIM resonator, which is in resonance with the incident

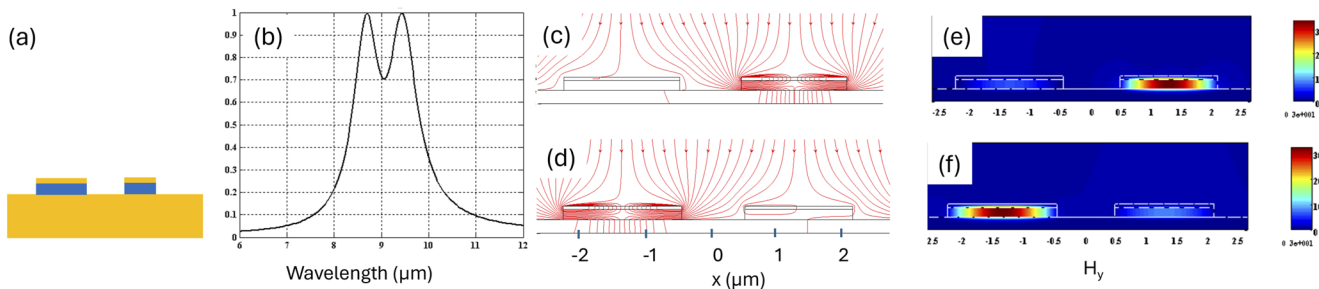


FIG. 4. Controlling the emission spectrum with MIM resonators. (a) Sketch of the periodic array of two MIM stripes with widths 1.78 and $1.62 \mu\text{m}$. The insulating spacer is ZnS and has a thickness of 152 nm . (b) Absorption spectrum with two different peaks at 8.7 and $9.44 \mu\text{m}$. (c) The lines of the Poynting vector of an incident plane wave at normal incidence at $8.7 \mu\text{m}$ are funneled toward the right MIM. (d) The lines of the Poynting vector of an incident plane wave at normal incidence at $9.44 \mu\text{m}$ are funneled toward the left MIM. The figure shows that the lines are funneled toward the lateral edges of the resonant MIM, enter the spacer, and penetrate the metal where absorption takes place. (e) The near-field distribution shows the enhancement of the magnetic field in the gap of the MIM resonator at $8.7 \mu\text{m}$. (f) The near-field distribution shows the enhancement of the field in the gap of the MIM resonator at $9.44 \mu\text{m}$. The permittivity of gold is given by a Drude model $\epsilon_r(\omega) = 1 - \omega_p^2/(\omega^2 + i\gamma\omega)$, where $\omega_p = 62\,893 \text{ cm}^{-1}$ and $\gamma = 302 \text{ cm}^{-1}$. The permittivity of ZnS is 4.84 .

field. In this example, we excite the fundamental mode of the MIM with a single antinode.

As discussed earlier, the size of the MIM resonator enables to control the central frequency of the resonance, and the critical coupling condition enables to achieve a unity emissivity. The remaining question is how to control the bandwidth of a resonator. As for any resonator, it is given by its quality factor and, therefore, the decay rate of the resonator. Given that the radiative decay rate should match the non-radiative decay rate due to metal and dielectric losses, it is the choice of the materials that enables to control the quality factor. Bad metals can be used for low quality factors, and metallo-dielectric structures replacing the MIM structure can be used for large quality factors.²⁹

B. Emission in a spectral band

Several applications such as radiative cooling³⁰ or infrared stealth³¹ require either emission in a given spectral band or multi-band emission. These bands are often dictated by the transparency windows of the atmosphere in the infrared, namely 3–5 μm or 8–13 μm . Single resonances cannot be used for these applications.

There are various strategies based on the MIM architecture in order to obtain band emission. The first one is to periodically repeat a cell containing several MIM resonators with different sizes leading to different absorption lines,²⁸ as illustrated in Fig. 4 for two resonators. The absorption bandwidth can be increased by adding more resonators shifted by an amount on the order of the spectral width of a single resonator.

Another possibility is to have a vertical stack of MIM resonators with linearly varying widths and, therefore, varying absorption frequencies. If the metallic layers are thin compared to the skin depth, the different modes are coupled, and the stack behaves as an equivalent sawtooth metamaterial exhibiting an ultrabroadband absorption.³² It is also possible to leverage several resonances in the MIM architecture by associating several harmonics of horizontal resonances as well as vertical resonances.³³

Alternatively, it is possible to use antireflection strategies with an absorbing material so that the energy penetrates the medium for frequencies in the antireflection bandwidth and is subsequently absorbed. According to Kirchhoff's law, emission is thus enhanced in the corresponding band. If the antireflection technique is broadband, the absorptivity and hence the emissivity are broadband. A simple approach to enhance absorption over a broadband is based on corrugated surfaces with correlation lengths larger than the wavelength so that multiple scattering increases absorption. An alternative mechanism is to use a grating with a sawtooth or quintic profile and a subwavelength period.³⁴ In this case, the corrugation can be viewed as an effective medium with a varying effective index, which prevents reflection.³⁵

Finally, photonic crystal structure can be used to generate a large reflectivity so that the absorption is reduced. Such a system can be obtained by designing a stack of alternating dielectric and metallic layers³⁶ or by etching a periodic array of holes in the material.³⁷

We finish with a brief comment on the state of the art. For all the systems discussed in this section, it is possible to obtain emission peaks with emissivity close to 1 at some frequencies. The most challenging issue is to reduce the residual emission away from the emitting peaks or emitting bands. A good figure of merit is the

fraction of emitted power that is emitted in the useful emission band.

V. TAILORING THE EMITTED POLARIZATION

According to Kirchhoff's law, the polarization state of an emitting thermal metasurface can be controlled via the polarization dependence of the device absorptivity. In the case of a plane interface between a lossy dielectric and vacuum, it is known that an incident impinging the surface close to the Brewster angle will be transmitted with no reflection for TM polarization, whereas the TE polarization will be partially reflected. Accordingly, the emission in TM polarization will be larger so that the body emits partially linearly polarized light at the Brewster angle. This is readily understood using the picture introduced in the discussion of Kirchhoff's law showing that emissivity is nothing but the interface transmission factor. Beyond this simple example, is it possible to engineer the polarization?

A possible approach is based on the concept of designing an intermediate mode to control the emission. We have introduced this idea to explain the directional emission mediated by a leaky surface mode. It is also possible to control the polarization of the emission by the same token. The first example is the emission by a grating ruled on an interface supporting a surface phonon polariton.^{19,38,39} This emission in the plane of propagation is TM polarized as the surface wave is TM polarized. A second approach is the emission by SiC whiskers,⁴⁰ which acts as a linear antenna and produces polarized radiation. A third approach is the emission of linearly polarized light using arrays of parallel absorbing (usually metallic) wires on a dielectric substrate. This is the typical structure used to design infrared polarizers in transmission. Light polarized along the wire direction is essentially absorbed, projecting the total polarization state onto the orthogonal direction. In the emission picture, random thermal currents flowing along wire-like structures are similar to currents driving a linear antenna.⁴¹

It is more difficult to produce the emission of circularly (or elliptically) polarized light. The fundamental reason is that circular polarization requires some degree of source current cross-correlation along two orthogonal directions, whereas random thermal currents along two directions are uncorrelated in an isotropic material. It is possible to shape linearly polarized light into circularly polarized light using retardation mechanisms inducing the appropriate phase relation between orthogonal polarization components. This can be performed to some extent, at a metasurface level. One can use, for instance, a passive metasurface placed atop an incandescent metasurface emitting linearly polarized light to mimicking in a compact fashion the free space, one-pass operation through a quarter-wave plate.⁴² Alternatively, for structures incorporating the contribution of two interfaces (typically in situations that involve using a back-reflecting mirror), superposition and interference of the directly emitted light and the back-reflected light, experiencing two passes through the metasurface, can be exploited to engineer the polarized emission.²³

According to Kirchhoff's law, designing a circularly polarized source is fundamentally tied to designing an absorber with strong circular dichroism. In other words, we want strong absorption contrast between left-circular and right-circular polarizations that are mirror-images of each other.⁴³ Therefore, more than inversion symmetry, mirror symmetry breaking is essential to ensure a total,

nonzero degree of circular polarization. Zigzags, spirals, or letters breaking mirror symmetry are reported in the literature as various shapes behaving as efficient chiral emitters.^{44,45}

Circularly polarized emission at the source level can be obtained by symmetry-breaking in the metasurface design. Broken inversion symmetry occurs when the structure geometry is not preserved under the $\mathbf{r} \rightarrow -\mathbf{r}$ operation, where \mathbf{r} is a position vector along the metasurface plane. Inversion asymmetry lifts the spin-degeneracy of surface waves—a phenomenon called the optical Rashba effect.⁴⁶ Two spin-dependent, momentum matching conditions coupling the surface waves to radiation can be written. Light of opposite chirality is emitted in opposite *oblique* directions away from the normal to the metasurface. Since these emission directions come in pairs, the net helicity summed over the entire far-field hemisphere remains zero.

Regarding the figure of merit, we use the Stokes vector,¹⁴ which can be evaluated by measuring intensities. ($S_0 = I_x + I_y$, $S_1 = I_x - I_y$, $S_2 = I_{45} - I_{-45}$, $S_3 = I_R - I_L$). A well-known quantity is the degree of polarization $\sqrt{S_1^2 + S_2^2 + S_3^2}/S_0$, which quantifies the fraction of the intensity that is polarized. The degree of circular polarization is given by S_3/S_0 . To obtain a large degree of polarization, it is necessary to avoid direct coupling to plane waves of the emitters. Instead, the coupling should be mediated by a mode that is fully polarized.

VI. TIME-MODULATION OF THERMAL EMISSION

Fast-modulation of thermal light would enable to increase the rate of information transmission via infrared light, and as such, is an important requirement of communication or detection applications. We have previously shown that the intensity emitted by a given body can be expressed as the product of its emissivity and the blackbody radiance, which only depends on the temperature. Hence, time-modulation of thermal emission can be, therefore, envisioned as achievable by means of either temperature modulation or emissivity modulation.⁴⁷

Temperature modulation sounds conceptually straightforward: it consists in switching on and off the heating of the emitting volume. Standard hot membranes can be modulated up to a few Hz. Their cooling rate is limited by thermal inertia.⁴⁸ This rate is dictated by the typical diffusion time of a material structure, given by $t = h^2/D$, where h is the typical structure dimension in the direction where we consider heat flux and D the material diffusivity, which is always typically of the order of $10^{-5} \text{ m}^2 \text{ s}^{-1}$. Achieving a fast modulation rate is, therefore, not fundamentally constrained by some intrinsic slowness of thermal diffusion but rather by the thickness of the emitting elements. This problem can be circumvented by using hot, thin emitters placed on a cold substrate,^{41,49} which serves as a heat sink. The emitters can cool in less than a microsecond, and modulation up to 10 MHz has been observed. Note that these devices are anisothermal, so their design requires the use of a local form of Kirchhoff's law.¹¹ Note also that the emission spectrum of such a source is no longer stationary as it changes with the time-dependent temperature. Although the emitting volume has to be thinner than 100 nm in order to enable a fast cooling by diffusion, it is possible to optimize its absorption so that the emissivity approaches 1.

The other possibility is to modulate the emissivity. This can be achieved in various ways. The idea shared by all approaches is to

exploit the dependence of the absorptivity with external parameters. Electrical modulation of emissivity is the first approach. All materials with numerous free electrons or more generally high mobility carriers, such as semiconductors, metals, graphene, and conductive oxides, can see their optical properties tuned by electrostatic gating as a general consequence of the modification of the carrier transport properties in regions of the material.^{50–52}

It is then interesting to add resonant phenomena in the picture to move toward time-modulated metasurfaces. In devices designed to achieve total absorption of light in a resonant mode of the system, thermal emission can be switched on or off by electrical control of this phenomenon. For instance, in the mid-IR, this method has been explored with stacks of quantum well films. The QW structure and material can be engineered to create a narrowband transition in this spectral range. The thermal metasurface can then be designed to maximize absorptivity and localize losses in the QW film.^{53,54} A modulation up to 600 kHz has been reported,⁵⁴ but the maximum temperature was limited by the materials used to less than 250 °C. Quantum wells based on GaN/AlGaN enabled them to reach 500 °C.⁵⁵

An alternative possibility to modulate emissivity is to use reconfigurable microelectromechanical systems (MEMS) to modulate the spectral emissivity. Emissivity modulation up to 110 kHz has been demonstrated with this scheme.⁵⁶ Emitting temperatures were limited in the range of 25–44 °C.

To conclude this section, let us note that emissivity can be modulated via thermal effects. Beyond thermo-optical effects in usual MIR materials, phase change materials have the ability to display a strong temperature dependent emissivity, making them interesting candidates as the base material to build a whole metasurface. Vanadium dioxide (VO_2) is one of these thermochromic materials, with its phase transition occurring between a dielectric phase and a metallic phase above 68 °C, inducing an increase in reflectivity and consequently a decrease in emissivity. Temperature-dependent emissivity is due, for a second class of materials, to transition from a crystalline phase to an amorphous phase with increasing temperature. Examples are chalcogenide based materials such as the well-known GST^{57,58} or perovskite based materials.⁵⁹ Interestingly, phase transitions in such non-volatile materials can be conveniently triggered and reverted using pulsed laser excitation, enabling the metasurface patterning and local control of the emission, in addition to time-modulation.⁶⁰

VII. TOWARDS HIGH EFFICIENCY THERMAL SOURCES

The efficiency of a thermal source η_{source} is given by the ratio between the useful radiated power and the input energy that was used to heat the thermal source itself. This efficiency can be split into three terms. First, the heating efficiency η_{heating} , second, the radiative efficiency η_{rad} that accounts for the competition between heat transfer processes, and then the useful part of the radiated energy η_{spec} that could include a limited spectrum, given a solid angle or a given polarization. The total efficiency is the product of these three terms that can be optimized independently, at least in a first step,

$$\eta_{\text{source}} = \eta_{\text{heating}} \eta_{\text{rad}} \eta_{\text{spec}}. \quad (14)$$

The heating efficiency $\eta_{heating}$ is given by the ratio between the energy needed to heat the thermal source and the external input energy. The most common way to heat a thermal source is by conduction with a hot plate or with optical or electrical input energy. While the former is not very efficient, it is useful in order to test the radiative efficiency or the useful radiation efficiency without extra steps of engineering. In contrast, optical or electrical control can lead to higher efficiencies. In the case of an electrical input energy, one has to account for the Joule losses that are not in the active part of the thermal source. An optical heating relies on the very high absorption of an input optical source (for instance, visible LEDs). Both approaches require an extra-step to engineer the heating mechanism of the thermal source (optical absorber or electrical contact with dissipative electrodes).

The radiative efficiency η_{rad} is given by the ratio of the radiative power to the total heat transfer power, which includes heat transfer from conduction and convection. For a given device, an obvious step to improve its radiative efficiency is to increase the temperature as the thermal emission scales as T^4 , while conduction and convection scales as T . However, material constraints limit (melting temperature, oxidation, and lifetime) to temperatures up to 1000 K in most cases, while even ultra-refractory materials have melting temperatures in the range of 3000 K. The key to large efficiency is the reduction of convection and conduction. Convection can be reduced by placing the emitter in vacuum. The remaining problem is conduction by the emitter holder. A proper design of the system can reduce significantly the conductive losses.⁶¹ Hence, there are no fundamental limits to the efficiency, which is practically limited by the quality of the thermal insulation of the hot emitter.

Finally, if we are interested in designing a source with a specified bandwidth and directivity, the efficiency η_{spec} is limited by the integral of the emitted power in unwanted directions and frequencies. Hence, it is seen that the efficiency is challenging for directional and narrowband emitters as emission must be suppressed over a large spectral and angular domain. For a source emitting in the visible and over all angles and polarization, a 40% luminous efficiency has been demonstrated.⁶²

VIII. BEYOND KIRCHHOFF'S LAW: EMISSION BY NON-RECIPROCAL MATERIALS

As discussed in Sec. II C, Kirchhoff's law essentially relies on the reciprocity of an interface, which results in a symmetric transmission factor. If one can make the transmission factor different, i.e., $T_{12} \neq T_{21}$, the interface will behave differently for the photons in the absorption and emission processes, resulting in an imbalance in emissivity E and absorptivity A . In fact, the transmission factor can be generalized to the scattering coefficients, and reciprocity implies a similar relationship for reflection factor R , i.e., $R_{12} = R_{21}$,⁶³ where 1 and 2 indicate the locations of the source and detector on the same side of the interface, respectively.

We can consider an emitter in blue shown in Fig. 5 and understand the implications of non-reciprocity for energy exchange between objects.⁶⁴ The emitter exchanges energy with two blackbodies denoted as 1 and 2 through two directions also labeled as 1 and 2, respectively. The system is at thermal equilibrium. Since the emissivity of the blackbody 1 in direction 1 is unity, and the emitted energy (E) is either absorbed (A) by the emitter or reflected

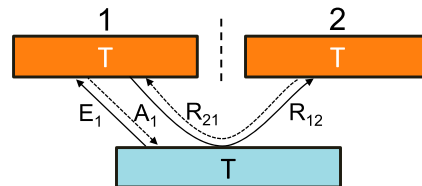


FIG. 5. A thermal emitter that exchanges energy with two blackbodies 1 and 2 through two directions. The emitter and the blackbodies are in thermal equilibrium.

(R) to the blackbody 2, one can obtain $A_1 + R_{12} = 1$. On the other hand, the absorbed energy by blackbody 1 is either from the emitter or from the emission of blackbody 2 and reflected by the emitter to 1. Therefore, we have $E_1 + R_{21} = 1$. For reciprocal systems, $R_{12} = R_{21}$, yielding $A_1 = E_1$. However, for nonreciprocal emitters, $R_{12} \neq R_{21}$ and, therefore, $A_1 \neq E_1$, breaking the conventional Kirchhoff's law.^{64–66}

The above discussion highlights two features of nonreciprocal thermal radiation. The first is that the net heat flow in a given direction can be nonzero even without a temperature difference. In the setup earlier, when considering both directions 1 and 2, the integrated net heat flow is zero since the system is in thermal equilibrium. However, the net heat flow is nonzero between each of the bodies in directions 1 and 2 due to the imbalance of the emitted and absorbed energy. The net nonzero heat flow leads to phenomena such as persistent heat current in multibody systems.⁶⁷ In nonthermal equilibrium systems, nonreciprocal thermal emission can lead to energy conversion at the thermodynamic limits, such as in solar energy harvesting^{68–70} and mechanical propulsion.⁷¹ The second implication is that for specular interfaces, though A and E are different for each individual direction, they may still be connected between different directions. In the above setup, for example, the same procedure can be conducted for direction 2, obtaining $A_2 = 1 - R_{21}$ and $E_2 = 1 - R_{12}$. Therefore, we still have $A_1 = E_2$. Such constraints are a result of compound symmetries,⁷² and one needs to break the symmetries to release these constraints.⁷³

Since reciprocity holds in linear, nonmagnetic, and steady systems,⁷⁴ one needs to introduce magnetic effects,^{64,75} time modulations,⁷⁶ or non-linearity⁷⁷ to the material system to achieve non-reciprocity. In magnetic systems, the motion of charged carriers is disturbed by an externally imposed magnetic field^{64,75} or the intrinsic magnetic effect.⁷⁸ For example, in magneto-optical materials, an external magnetic field triggers the cyclotron motion of electrons, yielding reciprocity breaking. Materials such as magnetic Weyl semimetals^{78,79} possess an internal magnetic effect and can exhibit strong non-reciprocity without an external magnetic field. Time modulation and nonlinear systems essentially seek to trigger asymmetric photonic band transitions for either absorbed or emitted photons, resulting in an imbalanced behavior.

With non-linearity, magnetic effect, or time modulation, bulk materials can exhibit non-reciprocity themselves, but the strength and bandwidth of the nonreciprocal effect can be significantly enhanced or tailored using the techniques discussed in Secs. III–VII, as shown in recent proposals using multilayer structures^{80,81} or grating structures.⁷⁵

IX. KIRCHHOFF'S LAW BEYOND THERMAL RADIATION

In Secs. III–VIII, we have seen that Kirchhoff's law plays a key role in the design of incandescent metasurfaces. In this section, we discuss the possibility of extending Kirchhoff's law beyond incandescence to apply it to photoluminescence and electroluminescence. As Kirchhoff's law provides an absolute formula for the emitted power, it should enable the design of light-emitting metasurfaces where external components such as collimators, filters, and polarizers would be integrated in a single device.

Let us first compare the similarities and differences between incandescence, electroluminescence, and photoluminescence. For the sake of simplicity, we will consider the case of light emission by a semiconductor. The quantum picture of the light emission process is the radiative recombination of an electron in the conduction band with a hole in the valence band. With this physical mechanism in mind, the only difference between incandescence, photoluminescence, and electroluminescence is the process to promote an electron of the valence band into the conduction band. It can be performed by heating (incandescence), absorbing incident photons (photoluminescence), or applying a voltage (electroluminescence) so that electrons are electrically injected in the conduction band. The emission process is the same: a photon is generated in the material by electron–hole recombination, and this photon has to be extracted from the semiconductor, namely transmitted by the interface between semiconductor and vacuum. The recombination process is the same for the three cases, so we expect Kirchhoff's law to be valid for these different processes. This is indeed the case when it is possible to assign a Fermi–Dirac distribution for the electrons in both bands with different Fermi levels called quasi-Fermi level. The difference between the two quasi-Fermi levels measures the strength of the pumping and is called photon chemical potential.⁸² Würfel has shown that the emitted power at frequency ω in direction \mathbf{u} with polarization l can be cast in the form⁸²

$$I_{\mathbf{u},\omega,l}^e(T) = A(-\mathbf{u},\omega,l) \frac{c}{8\pi} \times \frac{\omega^2}{\pi^2 c^3} \times \frac{\hbar\omega}{\exp[(\hbar\omega - \mu)/k_B T] - 1}, \quad (15)$$

where the absorptivity is computed in the presence of the pumping. It is seen that the key difference with incandescence is the introduction of a photon chemical potential μ in the Bose–Einstein distribution. In the case of electroluminescence, $\mu = eV$, where e is the modulus of the electrical charge of an electron and V is the applied voltage. This relation is valid in the presence of gain. The absorptivity then becomes a negative number for $\mu > \hbar\omega$. Note that the Bose–Einstein factor becomes also negative so that Eq. (15) is still valid in the gain regime.^{82,83}

We have seen that an incandescent emitter can be optimized by designing an emissivity close to 1. According to Eq. (15), emissivity (equal to absorptivity) is also the relevant figure of merit for photoluminescence and electroluminescence. A light-emitting photoluminescent metasurface has been demonstrated recently using a layer of nanoplatelets deposited on a silver metasurface by spin coating.⁸⁴ In this example, the absorptivity was on the order of 0.6%, and 40% of the emission was concentrated in a cone with a 15° aperture around the normal.

Let us stress the importance of using Kirchhoff's law to design the sources when using resonant metasurfaces. The usual procedure to design a light emitting device is to improve the spontaneous

emission by choosing the optimum semiconductor, designing heterostructures to promote electron–hole recombination, and enhancing this effect by enhancing the local density of states (Purcell factor). The second step is to optimize the extraction, namely, to ensure that photons emitted in the semiconductor are transmitted to the vacuum. The interplay between these two steps is thus not taken into account. When using Kirchhoff's law, the absorptivity is given by

$$A(-\mathbf{u},\omega,l) = \frac{1}{\epsilon_0 c |E_{inc}(-\mathbf{u},\omega,l)|^2} \int_V d^3\mathbf{r} \omega \epsilon_0 \text{Im}[\epsilon_r(\omega)] |E(\mathbf{r})|^2, \quad (16)$$

where V is the volume of the active material, $E_{inc}(-\mathbf{u},\omega,l)$ is the incident field illuminating the metasurface, and $E(\mathbf{r})$ is the induced field in the metasurface under this illumination. For a resonant metasurface, increasing the losses increases $\text{Im}[\epsilon_r(\omega)]$ but decreases the quality factor of the mode and, therefore, the value of the field in the volume V . Kirchhoff's law captures this interplay between enhancement of the field and enhancement of the intrinsic material absorption $\text{Im}[\epsilon_r(\omega)]$ in order to maximize the metasurface absorption A , which rules the emission.

X. CONCLUSION

Controlling incandescent sources with metasurfaces has been an active research field in the last decade. A recent review paper⁶ contains over 500 references. In this tutorial, we have attempted to provide a qualitative discussion of the principles involved in the design of incandescent metasurfaces. We hope that this text will be useful to clarify the key ideas and fundamental limits and serve as a conceptual guide for future developments.

Among the remaining issues to be addressed, we would like to stress that currently, most emitters are plagued by a background emission signal due to residual emissivity. Although many emitters display highly directional emission beams or very narrow emission peaks, there is still a broad background, both as a function of angle and frequency, that contains a significant part of the emitted power. Similarly, the polarized emission is still plagued by a non-polarized component. Another direction for future work is the development of active control of incandescence. Several works have reported time modulation of the intensity. Dynamic control of the emission frequency, the direction, and the polarization are also of interest. This topic merges with the emerging field of time-varying media, which has been recently explored for incandescent sources.⁸⁵

Finally, we have stressed that the control of emission that has been achieved in the field of incandescent sources can be extended to the design of photoluminescent and electroluminescent sources. While the development of incandescent sources has used Kirchhoff's law as a guide for the design, the development of visible light sources has been driven by separately optimizing the material for absorption on the one hand and the coupling to the vacuum modes (the extraction problem) on the other hand. The generalization of Kirchhoff's law to account for pumping should be very useful for the design of future sources. We stress that Kirchhoff's law can be used in the gain regime and account for effects such as spectral narrowing.⁸⁶ We also note that Kirchhoff's law can be used to model pulse emission, provided that a quasistationary approximation is valid. In practice, if the temperature and the photon chemical potential can be defined as a function of time, or in other words, for pulses longer than the

electron–phonon collision time and the electron–electron collision time, Kirchhoff's law should be applicable. It can also be used to model photoluminescence by metallic nanoparticles,⁸⁷ a nonequilibrium situation where the electronic distribution does not follow a Fermi–Dirac distribution. In conclusion, extending Kirchhoff's law to nonequilibrium systems leads to the development of a statistical physics theory of light emission.

ACKNOWLEDGMENTS

J.-J.G. acknowledges Jean-Paul Hugonin for preparing the figures used in Fig. 4. B.Z. acknowledges the support from the National Science Foundation under Grant No. CBET-2314210.

AUTHOR DECLARATIONS

Conflict of Interest

The authors have no conflicts to disclose.

Author Contributions

Jean-Jacques Greffet: Conceptualization (lead); Writing – original draft (lead); Writing – review & editing (lead). **Benjamin Vest:** Conceptualization (equal); Writing – original draft (equal); Writing – review & editing (equal). **Patrick Bouchon:** Conceptualization (equal); Writing – original draft (equal); Writing – review & editing (equal). **Bo Zhao:** Conceptualization (equal); Writing – original draft (equal); Writing – review & editing (equal).

DATA AVAILABILITY

Data sharing is not applicable to this article as no new data were created or analyzed in this study.

REFERENCES

1. Kirchhoff, "I. On the relation between the radiating and absorbing powers of different bodies for light and heat," *London, Edinburgh Dublin Philos. Mag. J. Sci.* **20**, 1–21 (1860).
2. W. Li and S. Fan, "Nanophotonic control of thermal radiation for energy applications [Invited]," *Opt. Express* **26**, 15995 (2018).
3. D. Baranov, Y. Xiao, I. Nechepurenko, A. Krasnok, A. Alù, and M. Kats, "Nanophotonic engineering of far-field thermal emitters," *Nat. Mater.* **18**, 920–930 (2019).
4. Y. Li, W. Li, T. Han, X. Zheng, J. Li, B. Li, S. Fan, and C.-W. Qiu, "Transforming heat transfer with thermal metamaterials and devices," *Nat. Rev. Mater.* **6**, 488–507 (2021).
5. M. Picardi, K. Nimje, and G. Papadakis, "Dynamic modulation of thermal emission—A tutorial," *J. Appl. Phys.* **133**, 111101 (2023).
6. J. E. Vazquez-Lozano and I. Liberal, "Review on the scientific and technological breakthroughs in thermal emission engineering," *ACS Appl. Opt. Mater.* **2**, 898 (2024).
7. Q. Chu, F. Zhong, X. Shang, Y. Zhang, S. Zhu, and H. Liu, "Controlling thermal emission with metasurfaces and its applications," *Nanophotonics* **13**, 1279–1301 (2024).
8. S. M. Rytov, Y. A. Kravtsov, and V. I. Tatarskii, "Principles of statistical radiophysics. 3," in *Elements of Random Fields* (Springer, New York, 1989).
9. H. Benisty, J.-J. Greffet, and P. Lalanne, *Introduction to Nanophotonics* (Oxford University Press, Oxford, 2022).
10. L. Landau, E. Lifshitz, and L. Pitaevskii, in *Statistical Physics Part I*, 1st ed., *Course of Theoretical Physics* (Pergamon, Amsterdam, 1980), Vol. 8.
11. J.-J. Greffet, P. Bouchon, G. Brucoli, and F. Marquier, "Light emission by nonequilibrium bodies: Local Kirchhoff law," *Phys. Rev. X* **8**, 021008 (2018).
12. J.-J. Greffet and M. Nieto-Vesperinas, "Field theory for generalized bidirectional reflectivity: Derivation of Helmholtz's reciprocity principle and Kirchhoff's law," *J. Opt. Soc. Am. A* **15**, 2735 (1998).
13. F. Marquier, K. Joulain, J.-P. Mulet, R. Carminati, and J.-J. Greffet, "Control spontaneous emission of light by thermal sources," *Phys. Rev. B* **104**, 155412 (2024).
14. C. Bohren and D. Huffman, *Absorption and Scattering of Light by Small Particles* (Wiley, New York, 1983).
15. S. Han and D. Norris, "Control of thermal emission by selective heating of periodic structures," *Phys. Rev. Lett.* **104**, 043901 (2010).
16. K. Joulain, J.-P. Mulet, F. Marquier, R. Carminati, and J.-J. Greffet, "Surface electromagnetic waves thermally excited: Radiative heat transfer, coherence properties and Casimir forces revisited in the near field," *Surf. Sci. Rep.* **57**, 59–112 (2005).
17. L. Mandel and E. Wolf, *Optical Coherence and Quantum Optics* (Cambridge University Press, Cambridge, 1995).
18. J. Goodman, *Statistical Optics* (Wiley, New York, 2000).
19. J.-J. Greffet, R. Carminati, K. A. Joulain *et al.*, "Coherent emission of light by thermal sources," *Nature* **416**, 61–64 (2002).
20. M. Zhou, E. Khoram, D. Liu, B. Liu, S. Fan, M. L. Povinelli, and Z. Yu, "Self-focused thermal emission and holography realized by mesoscopic thermal emitters," *ACS Photonics* **8**, 497–504 (2021).
21. H. Haus, *Waves and Fields in Optoelectronics, Prentice-Hall Series in Solid State Physical Electronics* (Prentice-Hall, 1984).
22. D. Costantini, A. Lefebvre, A.-L. Coutrot, I. Moldovan-Doyen, J.-P. Hugonin, S. Boutami, F. Marquier, H. Benisty, and J.-J. Greffet, "Plasmonic metasurface for directional and frequency-selective thermal emission," *Phys. Rev. Appl.* **4**, 014023 (2015).
23. A. Overvig, S. Mann, and A. Alù, "Thermal metasurfaces: Complete emission control by combining local and nonlocal light-matter interactions," *Phys. Rev. X* **11**, 021050 (2021).
24. I. Celanovic, D. Perreault, and J. Kassakian, "Resonant-cavity enhanced thermal emission," *Phys. Rev. B* **72**, 075127 (2005).
25. Z. Fan, T. Hwang, S. a. Lin *et al.*, "Directional thermal emission and display using pixelated non-imaging micro-optics," *Nat. Commun.* **15**, 4544 (2024).
26. I. Puscasu and W. L. Schaich, "Narrow-band, tunable infrared emission from arrays of microstrip patches," *Appl. Phys. Lett.* **92**, 233102 (2008).
27. X. Liu, T. Tyler, T. Starr, A. F. Starr, N. M. Jokerst, and W. J. Padilla, "Taming the blackbody with infrared metamaterials as selective thermal emitters," *Phys. Rev. Lett.* **107**, 045901 (2011).
28. P. Bouchon, C. Koechlin, F. Pardo, R. Haïdar, and J.-L. Pelouard, "Wideband omnidirectional infrared absorber with a patchwork of plasmonic nanoantennas," *Opt. Lett.* **37**, 1038–1040 (2012).
29. C. Blanchard, L. Wojszvyk, C. Jamois, J.-L. Leclercq, C. Chevalier, L. Ferrier, P. Viktorovitch, I. Moldovan-Doyen, F. Marquier, J.-J. Greffet, and X. Letartre, "Metallo-dielectric metasurfaces for thermal emission with controlled spectral bandwidth and angular aperture," *Opt. Mater. Express* **12**, 1–12 (2022).
30. A. P. Raman, M. A. Anoma, L. Zhu, E. Rephaeli, and S. Fan, "Passive radiative cooling below ambient air temperature under direct sunlight," *Nature* **515**, 540–544 (2014).
31. Y. Wu, S. Tan, Y. Zhao, L. Liang, M. Zhou, and G. Ji, "Broadband multispectral compatible absorbers for radar, infrared and visible stealth application," *Prog. Mater. Sci.* **135**, 101088 (2023).
32. Y. Cui, K. H. Fung, J. Xu, H. Ma, Y. Jin, S. He, and N. X. Fang, "Ultrabroadband light absorption by a sawtooth anisotropic metamaterial slab," *Nano Lett.* **12**, 1443–1447 (2012).
33. A. Cattoni, P. Ghenuche, A.-M. Haghiri-Gosnet, D. Decanini, J. Chen, J.-L. Pelouard, and S. Collin, " $\lambda/3/1000$ plasmonic nanocavities for biosensing fabricated by soft uv nanoimprint lithography," *Nano Lett.* **11**, 3557–3563 (2011).

³⁴W. H. Southwell, "Pyramid-array surface-relief structures producing antireflection index matching on optical surfaces," *J. Opt. Soc. Am. A* **8**, 549–553 (1991).

³⁵F. Ghmari and J.-J. Greffet, "Influence of microroughness on emissivity," *J. Appl. Phys.* **96**, 2656 (2004).

³⁶P. Dyachenko, S. Molesky, A. Petrov, M. Stormer, T. Krekeler, S. Lang, M. Ritter, Z. Jacob, and M. Eich, "Controlling thermal emission with refractory epsilon-near-zero metamaterials via topological transitions," *Nat. Commun.* **7**, 11809 (2016).

³⁷Y. Yeng, M. Ghebrebrhan, P. Bermel, W. Chan, J. Joannopoulos, M. Soljacic, and I. Celanovic, "Enabling high-temperature nanophotonics for energy applications," *Proc. Natl. Acad. Sci. U. S. A.* **109**, 2280 (2012).

³⁸N. Dahan, A. Niv, G. Biener, Y. Gorodetski, V. Kleiner, and E. Hasman, "Enhanced coherency of thermal emission: Beyond the limitation imposed by delocalized surface waves," *Phys. Rev. B* **76**, 045427 (2007).

³⁹G. Lu, C. R. Gubbin, J. R. Nolen, T. Folland, M. J. Tadjer, S. De Liberato, and J. D. Caldwell, "Engineering the spectral and spatial dispersion of thermal emission via polariton-phonon strong coupling," *Nano Lett.* **21**, 1831–1838 (2021).

⁴⁰J. A. Schuller, T. Taubner, and M. L. Brongersma, "Optical antenna thermal emitters," *Nat. Photonics* **3**, 658–661 (2009).

⁴¹L. Wojszvzyk, A. Nguyen, A.-L. Coutrot, C. Zhang, B. Vest, and J.-J. Greffet, "An incandescent metasurface for quasimonochromatic polarized mid-wave infrared emission modulated beyond 10 MHz," *Nat. Commun.* **12**, 1492 (2021).

⁴²S. L. Wadsworth, P. G. Clem, E. D. Branson, and G. D. Boreman, "Broadband circularly-polarized infrared emission from multilayer metamaterials," *Opt. Mater. Express* **1**, 466–479 (2011).

⁴³L. Ouyang, W. Wang, D. Rosenmann, D. A. Czaplewski, J. Gao, and X. Yang, "Near-infrared chiral plasmonic metasurface absorbers," *Opt. Express* **26**, 31484–31489 (2018).

⁴⁴A. Nguyen, J.-P. Hugonin, A.-L. Coutrot, E. Garcia-Caurel, B. Vest, and J.-J. Greffet, "Large circular dichroism in the emission from an incandescent metasurface," *Optica* **10**, 232–238 (2023).

⁴⁵X. Wang, T. Sentz, S. Bharadwaj, S. K. Ray, Y. Wang, D. Jiao, L. Qi, and Z. Jacob, "Observation of nonvanishing optical helicity in thermal radiation from symmetry-broken metasurfaces," *Sci. Adv.* **9**, eade4203 (2023).

⁴⁶N. Dahan, Y. Gorodetski, K. Frischwasser, V. Kleiner, and E. Hasman, "Geometric Doppler effect: Spin-split dispersion of thermal radiation," *Phys. Rev. Lett.* **105**, 136402 (2010).

⁴⁷J.-J. Greffet, "Controlled incandescence," *Nature* **478**, 191 (2011).

⁴⁸H. T. Miyazaki, T. Kasaya, H. Oosato, Y. Sugimoto, B. Choi, M. Iwanaga, and K. Sakoda, "Ultraviolet-nanoimprinted packaged metasurface thermal emitters for infrared CO₂ sensing," *Sci. Technol. Adv. Mater.* **16**, 035005 (2015).

⁴⁹C. Shi, N. H. Mahlmeister, I. J. Luxmoore, and G. R. Nash, "Metamaterial-based graphene thermal emitter," *Nano Res.* **11**, 3567–3573 (2018).

⁵⁰V. W. Brar, M. C. Sherrott, M. S. Jang, S. Kim, L. Kim, M. Choi, L. A. Sweatlock, and H. A. Atwater, "Electronic modulation of infrared radiation in graphene plasmonic resonators," *Nat. Commun.* **6**, 7032 (2015).

⁵¹G. T. Papadakis, B. Zhao, S. Buddhiraju, and S. Fan, "Gate-tunable near-field heat transfer," *ACS Photonics* **6**, 709–719 (2019).

⁵²N. H. Thomas, M. C. Sherrott, J. Brouillet, H. A. Atwater, and A. J. Minnich, "Electronic modulation of near-field radiative transfer in graphene field effect heterostructures," *Nano Lett.* **19**, 3898–3904 (2019).

⁵³S. Vassant, I. Moldovan Doyen, F. Marquier, F. Pardo, U. Gennser, A. Cavanna, J. L. Pelouard, and J. J. Greffet, "Electrical modulation of emissivity," *Appl. Phys. Lett.* **102**, 081125 (2013).

⁵⁴T. Inoue, M. D. Zoysa, T. Asano, and S. Noda, "Realization of dynamic thermal emission control," *Nat. Mater.* **13**, 928–931 (2014).

⁵⁵D. Kang, T. Inoue, T. Asano, and S. Noda, "Electrical modulation of narrowband GaN/AlGaN quantum-well photonic crystal thermal emitters in mid-wavelength infrared," *ACS Photonics* **6**, 1565–1571 (2019).

⁵⁶X. Liu and W. J. Padilla, "Reconfigurable room temperature metamaterial infrared emitter," *Optica* **4**, 430 (2017).

⁵⁷T. Cao, L. Zhang, R. E. Simpson, and M. J. Cryan, "Mid-infrared tunable polarization-independent perfect absorber using a phase-change metamaterial," *J. Opt. Soc. Am. B* **30**, 1580–1585 (2013).

⁵⁸Y. Qu, Q. Li, L. Cai, and M. Qiu, "Polarization switching of thermal emissions based on plasmonic structures incorporating phase-changing material Ge₂Sb₂Te₅," *Opt. Mater. Express* **8**, 2312–2320 (2018).

⁵⁹D. Fan, Q. Li, and P. Dai, "Temperature-dependent emissivity property in La_{0.7}Sr_{0.3}MnO₃ films," *Acta Astronaut.* **121**, 144–152 (2016).

⁶⁰P. Li, X. Yang, T. W. W. Maß, J. Hanss, M. Lewin, A.-K. U. Michel, M. Wuttig, and T. Taubner, "Reversible optical switching of highly confined phonon-polaritons with an ultrathin phase-change material," *Nat. Mater.* **15**, 870–875 (2016).

⁶¹G. Brucoli, P. Bouchon, R. Haider, M. Besbes, H. Benisty, and J.-J. Greffet, "High efficiency quasi-monochromatic infrared emitter," *Appl. Phys. Lett.* **104**, 081101 (2014).

⁶²O. Ilic, P. Bermel, G. Chen, J. Joannopoulos, I. Celanovic, and M. Soljacic, "Tailoring high-temperature radiation and the resurrection of the incandescent source," *Nat. Nanotechnol.* **11**, 320–324 (2016).

⁶³Z. Zhao, C. Guo, and S. Fan, "Connection of temporal coupled-mode-theory formalisms for resonant optical system and its time-reversal conjugate," *Phys. Rev. A* **99**, 033839 (2019).

⁶⁴L. Zhu and S. Fan, "Near-complete violation of detailed balance in thermal radiation," *Phys. Rev. B* **90**, 220301 (2014).

⁶⁵K. J. Shayegan, B. Zhao, Y. Kim, S. Fan, and H. A. Atwater, "Nonreciprocal infrared absorption via resonant magneto-optical coupling to InAs," *Sci. Adv.* **8**, eabm4308 (2022).

⁶⁶K. J. Shayegan, S. Biswas, B. Zhao, S. Fan, and H. A. Atwater, "Direct observation of the violation of Kirchhoff's law of thermal radiation," *Nat. Photonics* **17**, 891–896 (2023).

⁶⁷L. Zhu and S. Fan, "Persistent directional current at equilibrium in nonreciprocal many-body near field electromagnetic heat transfer," *Phys. Rev. Lett.* **117**, 134303 (2016).

⁶⁸M. A. Green, "Time-asymmetric photovoltaics," *Nano Lett.* **12**, 5985–5988 (2012).

⁶⁹Y. Park, B. Zhao, and S. Fan, "Reaching the ultimate efficiency of solar energy harvesting with a nonreciprocal multijunction solar cell," *Nano Lett.* **22**, 448–452 (2021).

⁷⁰S. Jafari Ghalekohneh and B. Zhao, "Nonreciprocal solar thermophotovoltaics," *Phys. Rev. Appl.* **18**, 034083 (2022).

⁷¹D. Gelbwaser-Klimovsky, N. Graham, M. Kardar, and M. Krüger, "Near field propulsion forces from nonreciprocal media," *Phys. Rev. Lett.* **126**, 170401 (2021).

⁷²C. Guo, B. Zhao, and S. Fan, "Adjoint Kirchhoff's law and general symmetry implications for all thermal emitters," *Phys. Rev. X* **12**, 021023 (2022).

⁷³B. Zhao, J. Wang, Z. Zhao, C. Guo, Z. Yu, and S. Fan, "Nonreciprocal thermal emitters using metasurfaces with multiple diffraction channels," *Phys. Rev. Appl.* **16**, 064001 (2021).

⁷⁴V. S. Asadchy, M. S. Mirmoosa, A. Díaz-Rubio, S. Fan, and S. A. Tretyakov, "Tutorial on electromagnetic nonreciprocity and its origins," *Proc. IEEE* **108**, 1684–1727 (2020).

⁷⁵B. Zhao, Y. Shi, J. Wang, Z. Zhao, N. Zhao, and S. Fan, "Near-complete violation of Kirchhoff's law of thermal radiation with a 0.3 T magnetic field," *Opt. Lett.* **44**, 4203–4206 (2019).

⁷⁶A. Ghaneendar, J. Wang, C. Guo, S. Fan, and M. L. Povinelli, "Nonreciprocal thermal emission using spatiotemporal modulation of graphene," *ACS Photonics* **10**, 170–178 (2022).

⁷⁷C. Khandekar, A. Pick, S. G. Johnson, and A. W. Rodriguez, "Radiative heat transfer in nonlinear Kerr media," *Phys. Rev. B* **91**, 115406 (2015).

⁷⁸B. Zhao, C. Guo, C. A. Garcia, P. Narang, and S. Fan, "Axion-field-enabled nonreciprocal thermal radiation in Weyl semimetals," *Nano Lett.* **20**, 1923–1927 (2020).

⁷⁹S. Pajovic, Y. Tsurimaki, X. Qian, and G. Chen, "Intrinsic nonreciprocal reflection and violation of Kirchhoff's law of radiation in planar type-I magnetic Weyl semimetal surfaces," *Phys. Rev. B* **102**, 165417 (2020).

⁸⁰Z. Zhang and L. Zhu, "Broadband nonreciprocal thermal emission," *Phys. Rev. Appl.* **19**, 014013 (2023).

⁸¹M. Liu, S. Xia, W. Wan, J. Qin, H. Li, C. Zhao, L. Bi, and C.-W. Qiu, "Broadband mid-infrared non-reciprocal absorption using magnetized gradient epsilon-near-zero thin films," *Nat. Mater.* **22**, 1196–1202 (2023).

⁸²P. Wurfel, "The chemical potential of radiation," *J. Phys. C: Solid State Phys.* **15**, 3967 (1982).

⁸³C. Henry and F. Kazarinov, "Quantum noise in photonics," *Rev. Mod. Phys.* **68**, 801 (1996).

⁸⁴E. Bailly, J.-P. Hugonin, J.-R. Coudeville, C. Dabard, S. Ithurria, B. Vest, and J.-J. Greffet, "2D silver-nanoplatelets metasurface for bright directional photoluminescence, designed with the local Kirchhoff's law," *ACS Nano* **18**, 4903–4910 (2024).

⁸⁵I. Liberal and N. Engheta, "Manipulating thermal emission with spatially static fluctuating fields in arbitrarily shaped epsilon-near-zero bodies," *Proc. Natl. Acad. Sci. U. S. A.* **115**, 2878–2883 (2018).

⁸⁶A. Loirette-Pelous and J.-J. Greffet, "On the applicability of Kirchhoff's law to the lasing regime," *Optica* (in press, 2024).

⁸⁷A. Loirette-Pelous and J.-J. Greffet, "Theory of photoluminescence by metallic structures," *ACS Nano* (in press, 2024).